Anomalous Electron Transport in Hall Thrusters: Electric Field Fluctuation Measurement

Kuwabara, Naoya
Department of Advanced Energy Engineering Science, Kyushu University

Chono, Masatoshi
Department of Advanced Energy Engineering Science, Kyushu University

Morita, Taichi
Department of Advanced Energy Engineering Science, Faculty of Engineering Science, Kyushu University

Yamamoto, Naoji
Department of Advanced Energy Engineering Science, Faculty of Engineering Science, Kyushu University

出版情報：Transactions of the Japan Society for Aeronautical and Space Sciences, Aerospace Technology Japan. 19 (1), pp.81-86, 2021-01-04. 日本航空宇宙学会
バージョン：

Trans. JSASS Aerospace Tech. Japan
Vol. 19, No. 1, pp. 81-86, 2021
DOI: 10.2322/tastj.19.81

Anomalous Electron Transport in Hall Thrusters: Electric Field Fluctuation Measurement

By Naoya KUWABARA,[1)] Masatoshi CHONO,[1)] Taichi MORITA,[1)] and Naoji YAMAMOTO[1)]

[1)]*Department of Advanced Energy Engineering Science, Kyushu University, Kasuga, Japan*

(Received July 12th, 2019)

Anomalous transport of electrons has considerable impact on the overall performance of Hall thrusters. Numerous studies have shown that high-frequency (on the order of MHz) fluctuations in both the electric field and plasma density are one of the causes of the anomalous transport. This phenomenon has yet to be measured in detail, however, because it is difficult to evaluate the density distribution of neutral particles and the dispersion relation of plasma oscillation in the several MHz range. It was therefore necessary to develop a device to measure the fluctuations in order to elucidate the cause of the anomalous transport. Here we focus on electric field fluctuations in the azimuthal direction inside a Hall thruster, and measure floating potential difference between two Langmuir probes. When a discharge current increases under a strong magnetic field, the azimuthal fluctuation in the frequency of 1-5 MHz is enhanced and fluctuations at ~100 kHz appear. These results suggest that azimuthal fluctuations in the electric field play an important role in the anomalous transport of electrons in the Hall thruster.

Key Words: Hall Thruster, Anomalous Transport, Fluctuation

Nomenclature

B	:	magnetic flux density, T
e	:	elementary charge, C
E_θ	:	azimuthal electric field, N/C
I_d	:	discharge current, A
I_ic	:	inner coil current, A
I_oc	:	outer coil current, A
m	:	mass, kg
$\dot{m}$	:	xenon mass flow rate, mg/s
V_d	:	discharge voltage, V
x	:	probe position, mm
μ	:	mobility, $\mathrm{m^2/Vs}$
ν	:	momentum collision frequency, Hz
τ	:	momentum collision period, s
ω	:	cyclotron frequency, Hz
Subscripts		
e	:	electron
r	:	radial direction

1. Introduction

Electric propulsion has attracted increased attention with the advent of small all-electric satellites. Among the electric propulsion devices currently in use or under consideration, Hall thrusters are expected to be widely used, because they offer many advantages, including high thrust power ratio. A Hall thruster will be installed, for example as the main engine of the Engineering Test Satellite IX (ETS9) under development by JAXA.[1)] Hall thrusters are compact because they have high thrust density and do not require a high voltage source for operation. Furthermore, a Hall thruster can achieve high thrust efficiency (more than ~50%) and high specific thrust (1,000-3,000 sec).[2,3)] These features make a Hall thruster suitable for near-earth missions such as attitude control and orbital transition.

Today's all-electric satellites often use ion thrusters, and require as much as six months to reach geostationary orbit, as their thrust power is inferior to chemical propulsion. Ideally, the time to achieve orbit should be on the order of three months, in order to decrease the likelihood of damage to the solar cells from cosmic rays, and to shorten the time to full operational functionality. For a three month window, however, the thrust power ratio would have to be increased to 90 mN/kW. A Hall thruster with high thrust power ratio could meet this need, with some improvement in the thrust power ratio. The anomalous transport of electrons is an important barrier to improving thrust power ratio, however; anomalous electron transport can increase the discharge current by a 20% without a commensurate increase in thrust, which results in a 20% reduction of thrust power ratio.

Numerous studies have been done and several hypotheses have been proposed on the causes of anomalous transport, including electron collision with channel walls and plasma oscillations (on the order of MHz) due to drift instability.[4,5)] However, the physical mechanism of this phenomenon has yet to be shown clearly. To investigate anomalous transport in detail it will be necessary to evaluate the density distribution of neutral particles inside the thruster and the dispersion relation of plasma oscillations in the MHz range, but such measurements have been difficult with existing technology. Therefore, in this study, we aim to measure plasma fluctuation in the azimuthal direction using two Langmuir probes to obtain some clarification of the process of anomalous electron transport.

2. Electron Diffusion

In a Hall thruster, ions are accelerated in the axial direction by the electric field, and the satellite is accelerated by the reaction force. Therefore, the electron current does not contribute to the net thrust. Furthermore, the external magnetic field in the radial direction hinder the electrons from moving towards an anode. However, the amount of electron diffusion becomes larger than the theoretical value calculated from classical diffusion theory when the magnetic field strength exceeds a certain value.[6] This phenomenon is called anomalous transport. This section describes the electron diffusion in detail.

2.1. Classical collisional transport

In general, some of the electrons collide with neutral particles and diffuse across the magnetic field lines. In classical diffusion theory, the electron mobility perpendicular to the magnetic field is written as Eq. (1).

$$\mu_{\mathrm{e}} = \frac{e}{m_{\mathrm{e}}\nu_{\mathrm{e}}}\frac{1}{1+(\omega_{\mathrm{e}}\tau_{\mathrm{e}})^2}, \tag{1}$$

where $\omega_e\tau_e$ (the Hall parameter) is written as Eq. (2).

$$\omega_{\mathrm{e}}\tau_{\mathrm{e}} = \frac{e}{m_{\mathrm{e}}\nu_{\mathrm{e}}}B\,. \tag{2}$$

These formulas mean that the electron diffusion is proportional to $1/B^2$. However, this does not agree well with experimental results in which the electron diffusion is proportional to 1/B.[7]

2.2. Anomalous transport

All of the electrons cannot be trapped by the magnetic field because collision of an electron with the wall or plasma fluctuations enhances the electron's mobility. The dominant cause of the anomalous transport is yet, however, clear. There has been experimental confirmation that the channel wall material plays a role in electron mobility.[8] Furthermore, electrons drift in the axial direction due to $\boldsymbol{E}_\theta \times \boldsymbol{B}_r$, where $\boldsymbol{E}_\theta$ is the azimuthal electric field produced by plasma fluctuations, and $\boldsymbol{B}_r$ is the applied magnetic field in the radial direction.[9-12] In fact, several simulation results have shown that fluctuations of azimuthal electric fields appear inside the thruster.[13,14] We experimentally measured the electric field fluctuations in the azimuthal direction, and investigated the relationship between the fluctuations and the electron transport.

3. Plasma Oscillation

Hall thrusters, in general, show complex behavior in their oscillation frequency over a wide range from kHz to GHz. These oscillations make the thruster unstable and contribute to the anomalous electron transport. Table 1 shows the oscillations observed inside a typical Hall thruster. These oscillations are categorized into five types according to frequency ranges.[2] The ionization oscillation comes from the density fluctuations between the neutral and charged particles. The amplitude of this oscillation is the largest among the five types oscillations, and this is the most important factor in the stability of the thruster.[15]

Table 1. Oscillation observed inside the thruster.

Oscillation	Frequency (kHz)
Ionization oscillation	10-10^2
Transit-time oscillation	10^2-10^3
Electron-drift oscillation	10^3-10^4
Electron-cyclotron oscillation	10^6
Langmuir oscillation	10^5-10^7

The transit-time oscillation is associated with the period in which an ion passes through the acceleration region. This amplitude depends on the magnetic field strength.[16]

As its name suggests, electron-drift oscillation is caused by the electron drift instability, which results from the density gradient in the acceleration channel. This instability is characterized by the growth of an azimuthal wave of wavelength in the mm range and with velocity on the order of the ion acoustic velocity. Some simulations have shown the presence of azimuthal electric field oscillations induced by electron drift instability.[17]

The electron-cyclotron oscillation results from the cyclotron motion of electrons, and the Langmuir oscillation results from electron inertia. These oscillations cannot be suppressed because they always exist in plasmas.[18]

4. Experiment

4.1. Experimental setup

In this study, a Langmuir probe was used to measure electric field fluctuations. The side and top views of the experimental setup are shown in Figs. 1 and 2, respectively. The probe was fixed on a linear actuator which was inclined at 45° to the exhaust plane as shown in Fig. 2. Measurements were performed at three positions, x = 3, 5 and 10 mm (with x being the distance from the tip of the probe to the origin, where x = 0). The origin is defined at the mid-height of the thruster, at the center of the channel width, and 1mm from the exhaust plane towards the anode.

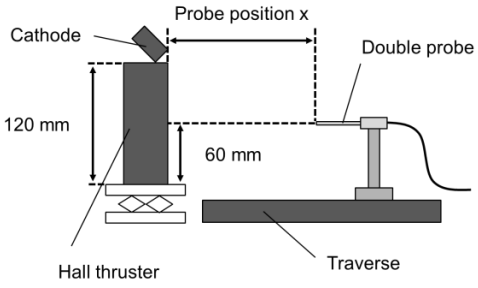

Fig. 1. Side view of the experimental setup.

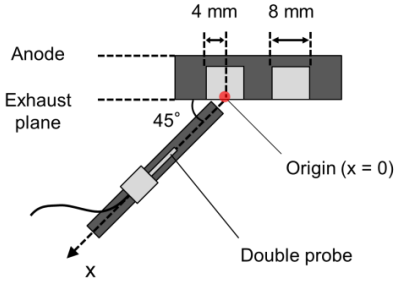

Fig. 2. Top view of the experimental setup.

4.2. Langmuir probe

The electric field fluctuation was evaluated by measuring the potential difference between the electrodes under the assumption of small temperature fluctuations,[19] since facility limitations prevent direct measurement of MHz plasma potential fluctuation. The validity of applying this assumption to high-frequency phenomenon and the frequency limitation of this measurement technique will be investigated in future work. A photograph of the Langmuir probe is shown in Fig. 3. This probe consists of two 0.15 mm diameter tungsten wires, which are covered with a 0.5 mm diameter ceramic tube except at the edge (1.5 mm in the lengthwise direction). The two electrodes are set at the medial of the acceleration channel, and separated in the azimuthal direction by 1 mm. It is possible to evaluate the electric field fluctuation by measuring the potential difference fluctuation because the electric field is the potential difference divided by the distance between the electrodes. The potential difference between the two probes is directly measured using a high-speed insulation module; this allows isolation difference voltage measurement (impedance 1 MΩ, capacitance 35 pF, accuracy 0.5%, and bandwidth DC - 20 MHz). A fast-Fourier-transform (FFT) was applied to the detected signal by the differential data recorder (bandwidth was less than 20 MHz under FFT analysis conditions, sampling rate 50 MS/s, record length 1 ms, and window function of the Hanning window).

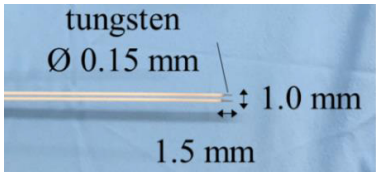

Fig. 3. Photograph of Langmuir probe.

4.3. Hall thruster

A magnetic layer-type Hall thruster (class 200 W) was used in this study. A schematic diagram of the exhaust plane is shown in Fig. 4 and a photograph of the Hall thruster is shown in Fig. 5. The acceleration channel is made of boron nitride, and the outer and inner diameters are 56 mm and 40 mm, respectively. The magnetic circuit is composed of five solenoid coils, one at the center of the thruster and the others outside the channel. When current is supplied to each coil, a radial magnetic field is created in the acceleration channel. The number of turns of the inner coil is two times larger than that of the outer coil. The ratio of the outer coil current to the inner coil current is one to two, that is, the magnetic field strengths produced by each coil are the same. The magnetic field strengths at inner coil current of 2.00 A are 16.2 mT (x = 3), 14.9 mT (x = 5) and 10.6 mT (x = 10). A 2D map of the magnetic flux density is described in Ref. 20). The typical plasma density is ~10^{18} m^3,[21] and electron temperature is 10 eV.

4.4. Cathode

The Hall thruster requires an electron source in front of the thruster to maintain the axial electric field and to neutralize the ion beam. In this study, a hollow cathode (HC252, Veeco Co.) was used as the electron source. The cathode is mounted on the thruster, tilted at 45 degree against the thruster axis, as shown in Fig.1. A hollow cathode emits electrons more stably and has longer life-time over 1000 hours than a filament cathode, although it requires an additional gas feed system. The propellant gas is ionized by collision with thermions emitted from a heated inserter (made of barium oxide and other materials with low work function).

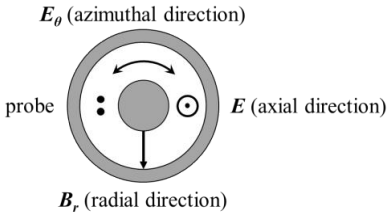

Fig. 4. Schematic diagram of the exhaust plane.

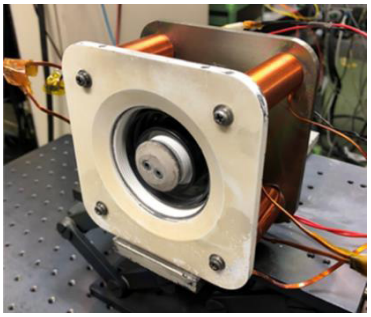

Fig. 5. Photograph of the Hall thruster.

4.5. Gas supply system

In this study, Xe gas (purity 99.9995%) was used both for the propellant of the Hall thruster and the driving gas of the hollow cathode. The mass flow rates were 1.0 mg/s and 0.27 mg/s for the thruster and cathode, respectively, and both flow rates were controlled independently. After the experiment, Ar gas (purity 99.999%) was used to cool the hollow cathode.

4.6. Vacuum facility

The experiment was conducted inside the vacuum chamber at Kyushu University. The inner diameter and the length of the vacuum chamber are 1.0 m and 1.2 m, respectively. The pumping system consists of a rotary pump (pumping speed: 8.7×10^{-2} m^3/s), a mechanical booster pump (pumping speed: 1.0×10^{-1} m^3/s), two turbo molecular pumps (pumping speed: 2.2×10^{-1} m^3/s and 1.9×10^{-1} m^3/s), and a cryogenic pump (pumping speed: 2.0 m^3/s). The chamber baseline pressure is below 3.4×10^{-4} Pa, and the pressure during thruster operation is below 7.3×10^{-3} Pa.

5. Results and Discussion

5.1. Discharge current oscillations

The trajectory of the discharge current with respect to change in inner coil current is shown in Fig. 6. This figure shows a typical trajectory of the discharge current; the value of the discharge current gradually decreases as the channel wall temperature increase over time. In this experiment, when the inner coil current increased up to 1.45 A, the discharge current was suppressed in inverse proportion to the inner coil current. In other words, electron diffusion is most suppressed at the inner coil current 1.45 A and discharge current 0.54 A,

as shown in Fig. 6. However, when the inner coil current exceeds 1.45 A, the discharge current increases sharply. Thus, the discharge current is 0.65 A at inner coil current 2.00 A. This would be caused by anomalous transport. The electron diffusion is in "classical diffusion mode" when the inner coil current is below 1.45 A, and it is in "anomalous transport mode" over 1.45 A.

Next, we show discharge current oscillations in the Hall thruster used in this study. The discharge current was measured by a current probe (TCP312, Tektronix Co.). Figures 7(a)-7(c) show the FFT spectrum of the discharge current at discharge voltage of 150 V and inner coil current of 1.45 A and 2.00 A (from 1 to 15,000 kHz). As shown in Fig. 7(a), the ionization oscillation shows the largest peak. The transit-time oscillation has a broad band spectrum while the electron-drift oscillation has a narrow band spectrum. Compared to the discharge current oscillations at inner coil current of 1.45 A (classical diffusion mode), the amplitudes of 100-300 kHz oscillation (assumed to be transit-time oscillation) and 1,000-3,000 kHz oscillation (assumed to be electron-drift oscillation) at inner coil current of 2.00 A (anomalous transport mode) are large. On the other hand, the ionization oscillation dominates at inner coil current of 1.45 A (classical diffusion mode) and other oscillations are suppressed.

Figure 7(c) shows the FFT spectrum of the discharge current at inner coil current of 1.45 A and probe position is 120 mm downstream of the thruster exit. The discharge current spectrum of 7(a) (x = 3 mm) is almost the same as that of 7(c), showing that the perturbation caused by inserting the probe can be ignored. Thruster operation was stopped when the probe moved to within 3 mm of the exit.

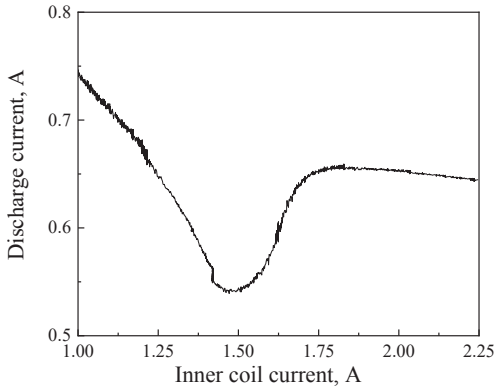

Fig. 6. Trajectory of the discharge current with respect to change in inner coil current.

5.2. Azimuthal electric field fluctuation

The time history of the azimuthal electric field estimated from the difference in floating potential at discharge voltage of 150 V and inner coil current of 2.00 A is shown in Fig. 8. The electric field fluctuates at 1 MHz with 20 kHz beating, and the amplitude of the fluctuation is the order of 10^2 V/m. Figures 9(a)-9(f) show the FFT spectra from 1 to 15,000 kHz measured at x = 3 mm [Figs. 9(a) and (b)], 5 mm [Figs. 9(c) and (d)] and 10 mm [Figs. 9(e) and (f)] with two different currents of the inner coil (1.45 A and 2.00 A). We compared the electric field fluctuations in the classical diffusion mode (I_{ic} = 1.45 A) and the anomalous transport mode (I_{ic} = 2.00). The operating conditions were I_{ic} = 1.45 A, I_{oc} = 2.90 A, V_d = 150 V and I_d = 0.58 A for the classical diffusion mode, and I_{ic} = 2.00 A, I_{oc} = 4.00 A, V_d = 150 V and I_d = 0.68 A for the anomalous transport mode.

As shown in Figs. 7 and 9, three types of fluctuations were measured by the probe, and their frequencies were in good agreement with the frequency of the discharge current oscillations. The largest discharge current oscillation amplitude is several tens of kHz, and the largest amplitude of potential difference fluctuation is 1-5 MHz. The fluctuations at frequency range of 1-5 MHz might be drift instability; the dispersion relation of this oscillation will elucidate the cause of this oscillation, we will address it in future work. The fluctuations have a peak value near 3 MHz. Although the frequency of this peak is the same in every case, the amplitude changes depending on the magnetic field strength. We fitted FFT spectra of the potential difference in Fig. 9 with the Lorentz function to estimate the peak value of the oscillation amplitude in the 0.9-15 MHz range. Figure 10 shows the peak value of the potential difference fluctuation estimated with the Lorenz fitting (from 0.9 to 15 MHz) in each probe position. As shown in Fig. 10, the peak value of the anomalous transport mode oscillation is larger than that of the classical diffusion mode oscillation. This means that the electric field fluctuation in the azimuthal direction in the anomalous

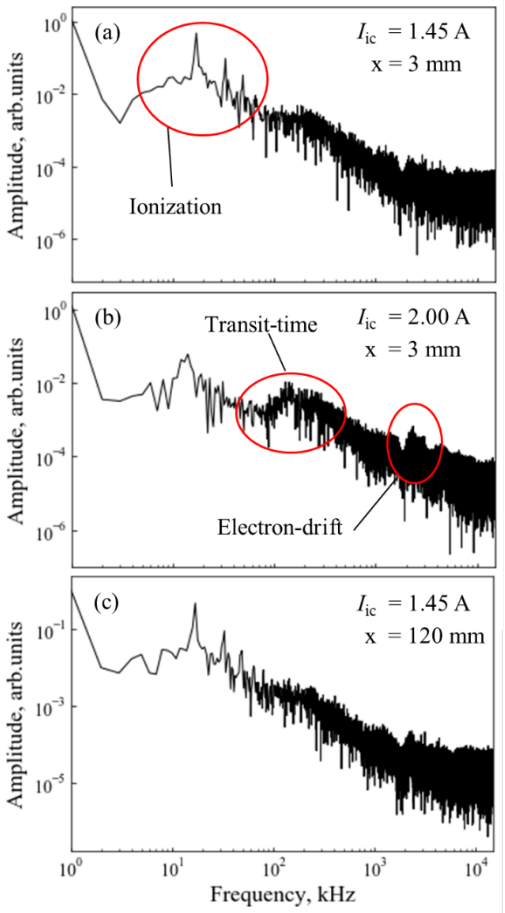

Fig. 7. FFT spectrum of the discharge current at discharge voltage of 150 V and inner coil current of 1.45 A and 2.00 A (from 1 to 15,000 kHz).

transport mode is larger than that in the classical diffusion mode. That is, the azimuthal electric field fluctuation affects electron diffusion or the electron anomalous transport affects the azimuthal electric field. Furthermore, it can be seen that the peak value of the fluctuation in the classical diffusion mode decreases as the probe approaches the thruster. This fluctuation is considered to be derived not only from the azimuthal fluctuation but also from the other instabilities. One candidate source of instability is the ion acoustic turbulence in the vicinity of the hollow cathode located outside the thruster. Several studies have considered the noise from hollow cathodes, and it has been found that hollow cathodes generate noise in the MHz band.[22,23] In fact, the characteristic oscillations at the same level as classical diffusion mode oscillations are observed while the thruster is not operating and only the hollow cathode is powered. This oscillation disappears when the hollow cathode is turned off. The hollow cathode is inclined toward the downstream to neutralize the ion beam, so the effect of the instability deduced from the cathode is reduced as the probe approaches the thruster because the distance from the probe to the outlet of the cathode increases. In the future, several probes will be arranged in the azimuthal direction to examine in more detail the spatial structure of the electric field fluctuations and the influence of the hollow cathode.

The other oscillations also change depending on condition. Ionization oscillation has a peak value near 10 kHz, and its narrow peak in the classical diffusion mode becomes broader in the anomalous transport mode. Comparing Figs. 9(a) and 9(b), the transit-time oscillation is clearly observed only in the anomalous transport mode. The reason for this spectral difference is not clear from the present measurement.

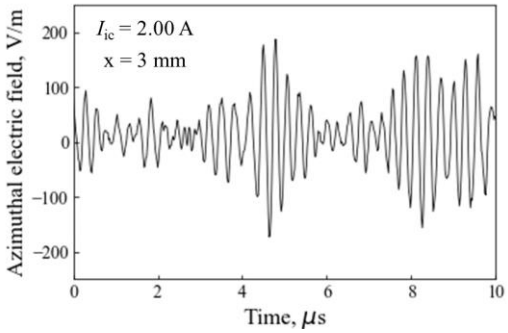

Fig. 8. Time history of the azimuthal electric field estimated from the difference in floating potential at discharge voltage of 150 V and inner coil current of 2.00 A (from 0 to 10 μs).

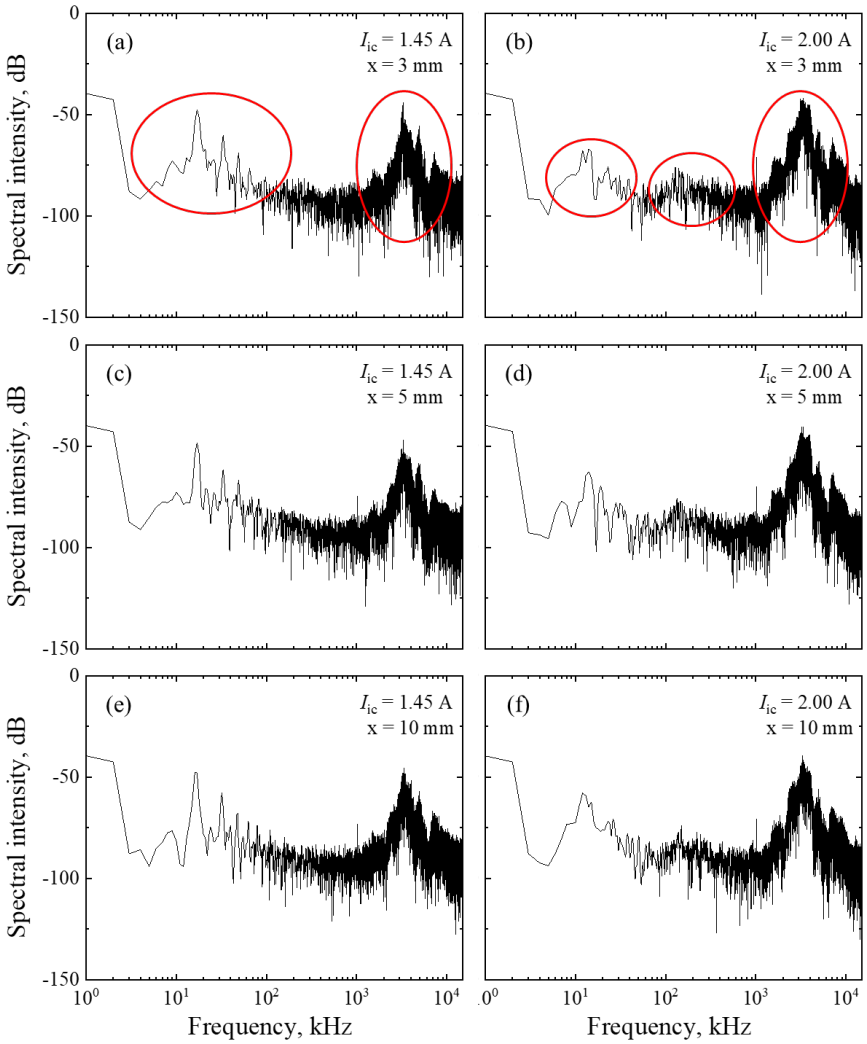

Fig. 9. FFT spectra of the potential difference (from 1 to 15,000 kHz). Comparison of the potential difference fluctuation with both classical diffusion mode (I_{ic} = 1.45 A) and anomalous transport mode (I_{ic} = 2.00 A). In each mode, measurement was performed at three positions, x = 3, 5 and 10 mm.

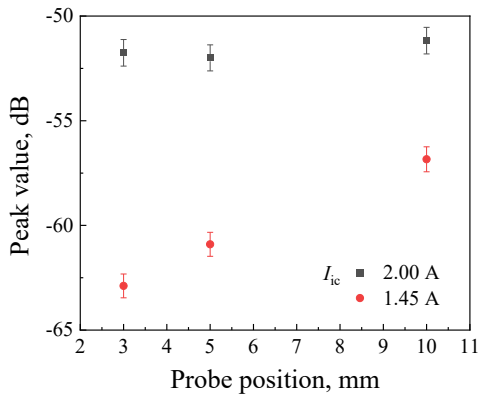

Fig. 10. Peak value of the potential difference fluctuation calculated by the Lorenz fitting in each probe position (from 0.9 to 15 MHz).

6. Conclusion

In this work, we have observed frequency response in azimuthal electric field fluctuations for two modes: the classical diffusion mode and the anomalous transport mode. The fluctuation in the MHz band is dominant, and its amplitude is larger in the anomalous transport mode. This indicates that the MHz band electric field fluctuation in the azimuthal direction greatly affects electron diffusion or electron diffusion mode affects the MHz band fluctuation. In addition, the magnitude of the amplitude in the MHz band decreases as the probe approaches the thruster, perhaps due to the effect of ion acoustic oscillation from the hollow cathode. In future work, by stationing multiple probes in the azimuthal, radial, and axial directions, we will investigate the spatial fluctuation of the electric field and the spread of ion acoustic oscillations from the hollow cathode. In the present experiment, the transit-time oscillation around 100 kHz is seen clearly only in the anomalous transport mode. Numerical simulation will be used to determine why this oscillation is large only in the anomalous transport mode.

Acknowledgments

This work was supported by JSPS KAKENHI Grant Number JP18H03815, Mitsubishi Electric Corporation, and JAXA.

References

1) Funaki, I., Cho, S., Sano, T., Fukatsu, T., Tashiro, Y., Shiiki, T., and Nakamura, Y.: Status Report on the Development of a Hall Thruster for Japanese All-Electric Propulsion Satellite, *The Japan Society for Aeronautical and Space Sciences*, **66** (2018), pp. 346-351 (in Japanese).
2) Choueiri, E. Y.: Plasma Oscillations in Hall Thrusters, *Physics of Plasmas*, **8** (2001), pp. 1411-1426.
3) Fukushima, Y., Yokota, S., Komurasaki, K., and Arakawa, Y.: Discharge Stabilization for an Anode-Layer-Type Hall Thruster by Azimuthally Nonuniform Propellant Supply, *The Japan Society for Aeronautical and Space Sciences*, **58** (2010), pp. 8-14 (in Japanese).
4) Bugrova, A. I., Morozov, A. I., and Kharchevnikov, V. K.: Experimental Investigation of Near Wall Conductivity, *Sov. Phys. Tech. Phys*., **16** (1990), pp. 849-856.
5) Kawashima, R., Hara, K., and Komurasaki, K.: Numerical Analysis of Azimuthal Rotating Spokes in a Crossed-field Discharge Plasma, *Plasma Sources Science and Technology*, **27** (2018), 035010.
6) Yamamoto, N., Nakagawa, T., Komurasaki, K., and Arakawa, Y.: Discharge Plasma Fluctuations in Hall Thrusters, *Vaccum*, **65** (2002), pp. 375-381.
7) Yoshikawa, S., Rose, D. J.: Anomalous Diffusion of a Plasma Across a Magnetic Field, *The Physics of Fluids*, **5** (1962), pp. 334-340.
8) Boeuf, J. P.: Tutorial: Physics and Modeling of Hall Thrusters, *J. Applied Physics*, **121** (2017), pp. 011101-1-011101-24.
9) Lafleur, T., Baalrud, S. D., and Chabert, P.: Theory for the Anomalous Transport in Hall Effect Thrusters. I. Insights from particle-in-cell simulations, *Physics of Plasmas*, **23** (2016), pp. 053502-1-053502-11.
10) Morozov, A. I., Esipchuk, Yu. V., Kapulkin, A. M., Nevrovskii, V. A., and Smirnov, V. A.: Azimuthally Asymmetric Modes and Anomalous Conductivity in Closed Electron Drift Accelerators, *Sov. Phys. Tech. Phys*., **18** (1973), pp. 615-620.
11) Reza, M., Faraji, F., Andreussi, T., and Andrenucci, M.: A Model for Turbulence-Induced Electron Transport in Hall Thrusters, 35th International Electric Propulsion Conference, Georgia, USA, IEPC-2017-367, 2017.
12) Hara, K.: Progress of Theory and Simulation on Ionization Oscillations in Hall Effect Thrusters, *J. Plasma and Fusion Research*, **94** (2018), pp. 475-481 (in Japanese).
13) Hirakawa, M., Arakawa, Y.: Particle Simulation of Plasma in Electric Propulsion Thrusters, *The Japan Society for Aeronautical and Space Sciences*, **45** (1997), pp. 444-452 (in Japanese).
14) Arakawa, Y., Komurasaki, K., and Hirakawa, M.: Hall Thruster, *The Japan Society for Aeronautical and Space Sciences*, **46** (1998), pp. 146-153 (in Japanese).
15) Boeuf, J. P., Garrigues, L.: Low Frequency Oscillation in a Stationary Plasma Thruster, *J. Applied Physics*, **84** (1998), pp. 3541-3554.
16) Vaudolon, J., Mazouffre, S.: Investigation of the Ion Transit Time Instability in a Hall Thruster Combining Time-Resolved LIF Spectroscopy and Analytical Calculations, 34th International Electric Propulsion Conference, Hyogo, Japan, IEPC-2015-400, ISTS-2015-b-400, 2015.
17) Boeuf, J. P., Garrigues, L.: E × B Electron Drift Instability in Hall Thrusters: Particle-in-Cell Simulations vs. theory, *Physics of Plasmas*, **25** (2018), pp. 061204-1-061204-15.
18) Chen, F. F.: *Introduction to Plasma Physics and Controlled Fusion,* Plenum Press, New York, 1974, pp. 82-86.
19) Ratynskaia, S. V., Demidov, V. I., and Rypdal, K.: Probe Measurements of Low-Frequency Plasma Potential and Electric Field Fluctuations in a Magnetized Plasma, *Physics of Plasmas*, **9** (2002), pp. 4135-4143.
20) Chono, M., Yamamoto, N., Morishita, T., Tsukizaki, R., Kubota, K., Kinefuchi, K., and Takahashi, T.: Development of a 200 W Class Hall Thruster for an Active Debris Removal System, 36th International Electric Propulsion Conference, Vienna, Austria, IEPC-2019-557, 2019.
21) Kuwabara, N., Chono, M., Yamamoto, N., and Kuwahara, D.: Plasma Fluctuations Measurements in a Hall Thruster, 36th International Electric Propulsion Conference, Vienna, Austria, IEPC-2019-665, 2019.
22) Jorns, A. M., Mikellides, G. I., and Goebel, D. M.: Ion Acoustic Turbulence in a 100-A LaB_6 Hollow Cathode, *Physical Review E*, **90** (2014), pp. 063106-1-063106-10.
23) Nishiyama, K., Shimizu, Y., Funaki, I., Kuninaka, H., and Toki, K.: Electromagnetic Noise from a Microwave Discharge Neutralizer and a Hollow Cathode, *The Japan Society for Aeronautical and Space Sciences*, **49** (2001), pp. 84-91 (in Japanese).